Scanning Microscopy

Volume 6 | Number 1 Article 3

1-27-1992

Integrated Single Crystal Detector for Simultaneous Detection of Cathodoluminescence and Backscattered Electrons in Scanning Electron Microscopy

Rudolf Autrata
Czechoslovak Academy of Sciences

Josef Jirák
Technical University, Brno

Jiří Špinka
Technical University, Brno

Otakar Hutař
Technical University, Brno

Scanning Microscopy, Vol. 6, No. 1, 1992 (Pages 69-79) 0891-7035/92$5.00+.00
Scanning Microscopy International, Chicago (AMF O'Hare), IL 60666 USA

INTEGRATED SINGLE CRYSTAL DETECTOR FOR SIMULTANEOUS DETECTION OF CATHODOLUMINESCENCE AND BACKSCATTERED ELECTRONS IN SCANNING ELECTRON MICROSCOPY

Rudolf Autrata[1*], Josef Jirák[2], Jiří Špinka[2], Otakar Hutař[2]

1: Institute of Scientific Instruments,
Czechoslovak Academy of Sciences, Brno, Czechoslovakia
2: Department of Electrotechnology, Faculty of Electrical Engineering,
Technical University, Brno, Czechoslovakia

(Received for publication May 17, 1991, and in revised form January 27, 1992)

Abstract

The design of the majority of the available high efficiency cathodoluminescence (CL) detection systems allows the secondary electron (SE) and backscattered electron (BSE) image modes to be detected simultaneously to a limited degree only. The described CL-BSE detector is based on the single crystal YAG scintillator shaped as a spherical mirror which reflects photons emitted from the CL specimen and focuses them on to the entrance surface of a fibre optic light guide connected to the photomultiplier tube (PMT I). The backscattered electrons emitted from the CL specimen move through the reflecting layer of the mirror into the YAG scintillator where they are transformed into photons and guided using a fixed light guide to the PMT II. This allows the simultaneous recording of CL and BSE image modes without changing the specimen position. The detector design does not obstruct the simultaneous detection of SEs by the conventional SE detector. The examples of the simultaneous CL, SE and BSE detection given demonstrate deeper understanding of the specimens properties in different fields of science.

Key Words: Scanning electron microscopy, cathodoluminescence, secondary electron image, backscattered electron image, single crystal, yttrium aluminium garnet, collecting system.

***Address for correspondence:**
Rudolf Autrata,
Institute of Scientific Instruments,
Czechoslovak Academy of Sciences,
Královopolská 147, 612 64 Brno, Czechoslovakia
Phone No: 42-5-749292, Fax No: 42-5-752765

Introduction

Light emission caused by the interaction of electrons with organic or inorganic matter is called cathodoluminescence (CL).

The biggest problem connected with the CL imaging is the low CL intensity of most substances in the range of electron beam currents currently used in SEM, i.e. in the range of currents at which a relatively satisfactory spatial resolution is achieved. The CL intensity of organic substances, especially the biological ones, is even by several orders lower than that of inorganic phosphors. The use of higher electron beam currents (e.g.>10^{-9}A) for the excitation of a higher CL emission leads not only to a decrease in resolution, but also to a rapid destruction of organic specimens and sometimes to a decrease in the CL intensity of inorganic specimens.

A number of authors tried to solve this problem by constructing efficient apparatuses to allow the detection of very low light levels. Most of them are very complicated and very expensive devices for which adaptations in the microscope must be made.

The simplest apparatus for the recording of the integral CL, which is the most frequently used CL mode, must include a light collecting system, a light detector and an amplifier with the video amplifier of the SEM. The light collecting system is the most important part of the CL chain and was, therefore, discussed by many authors. One of the cheapest and simplest systems is the light pipe collecting system (Barnett et al. 1975, Davidson et al. 1975, Jones and Gopinath 1973) that has, unfortunately, a low efficiency and a small solid angle of photon collection that is rarely larger than 0.5 steradians. But technically more complicated lenses have a similar angle (Williams and Yoffe 1969, Thornton 1968).

A substantial increase in the light collection efficiency was achieved by using ellipsoidal (Hörl and Mügschl 1972, Carlsson and Essen 1974, De Mets 1974) or parabolic (Jones and Gopinath 1973, Judge et al. 1974, Bond et al. 1974) mirrors in connection with fibre optic light guides. For spectral CL, the light reflected by the mirrors can be focussed on the spectrometer (Balk et al. 1975, Rasul and Davidson 1977, McKinney and Hough 1977). An extensive review of light collecting

systems and their applications for CL imaging was presented by Hörl (1978) and by Herbst and Hoder (1978). The bibliography of CL was written by Bröcker and Pfefferkorn (1978).

Disadvantages of recent systems

All light collecting systems based on ellipsoidal and parabolic mirrors have a high collection efficiency (see Table 1 in Vale and Greer 1977) that is indispensable for a precise study of substances in the spectral CL mode, but their construction is rather complicated, which is a disadvantage to those users of SEM to whom the CL image should serve as a complementary mode only.

Moreover, ellipsoidal and parabolic mirrors with their wide angle of photon collection, create a mechanical obstacle to an efficient collection of secondary (SE) or backscattered electrons (BSE). To facilitate their escape from the specimen toward the SE or BSE detector, it is necessary to make a sufficiently large hole. On the one hand, this hole decreases the efficiency of photon collection and, on the other hand, it affects the extraction of signal electrons. Except low efficiency light guides or lens CL detectors, no CL detection system allows the simultaneous detection of SE, BSE and CL in real time.

Different mechanisms of generation of BSEs and X-rays emitted from different specimen depths (in the dependence on the primary electron beam energy) supply information about the specimen that is quite different from that provided by CL. If the identification of the investigated specimen is to be as complete as possible, it is necessary to record all information modes at one time with a high efficiency, without changing the specimen position. A certain degree of compromise will probably always be necessary.

So far the best compromise solution regarding the simple design of the CL collecting system, its economy, relatively high efficiency and a possibility of implementing the simultaneous detection of CL and BSEs was presented by Boyde and Reid (1983a, 1983b). The CL collecting system consists of an aluminium (Al) foil tube whose one end (its shape resembles the paraboloid) is connected to the specimen and acts as a reflector of light toward the light guide, and the other end is connected to the light guide rod. This "clever" design has found strong acceptance in large volume applications in the user field. But it has also some disadvantages. If a solid state detector is used for the detection of BSEs, the Al tube bore must have a large diameter, which leads to a decrease in the solid angle of collection of CL light. (According to our measurement results, a 15 mm diameter bore leads to a decrease in collection efficiency by 30 %). Since the BSEs hit the light guide (which is more or less cathodoluminescent) directly, the BSE signal participates in the CL image. It is not possible to implement the simultaneous detection of BSE, SE and CL in real time because the SE detector is removed if the Al tube collector is used. Moreover, SEs can be extracted only if another hole is made in the Al tube or if the specimen is partially drawn out from the tube or the tube is removed.

Some time ago Boyde (private communication) suggested to integrate the BSE detector with the CL light reflector. The authors of this article seized upon that idea and built a detector described here.

Instrumentation for CL-BSE detection

The basic part of the integrated CL-BSE detector is the scintillation single crystal of yttrium aluminium garnet activated by cerium ($YAG:Ce^{3+}$) that is shaped as a concave spherical lens (Fig. 1) with a radius of curvature of 32.5 mm, diameter of 29.9 mm and has a 3 mm hole in its centre to allow the passage of primary electrons. The crystal is glued into the light guide made of organic glass. The highly polished spherical surface of the scintillation crystal is covered with a 70 nm opaque layer of aluminium creating a mirror with a reflectivity of 84 %. The remaining surfaces of the scintillation crystal and the part of the light guide touching the crystal are covered with a 200 nm thick aluminium layer. In addition to this, the entire surface of the scintillation crystal, with the exception of the mirror, is covered with an aluminium foil. This thorough shielding should ensure that not a single photon generated by the incident BSEs can be emitted from the crystal into the outer space.

The scintillation crystal with the light guide lies on the bottom base of the pole-piece of the microscope. The specimen of maximum size 5 x 5 mm is mounted to the specimen stub by using a bent metal rod ("gallows"). At a certain distance below the specimen, the window of the fibre optic light guide (ϕ 13 mm) is positioned on the axis of the primary beam and into this window the photons reflected by the spherical mirror are focussed. The fibre optic light guide is fixed either in the opening intended for the specimen stub or in a suitable place of the stage.

The photons generated in the CL specimen and reflected by the spherical mirror of the scintillation crystal into the window of the fibre optic light guide are propagated toward the photocathode of PMT II. At the same time, the incident BSEs hit the mirror of the scintillation crystal, pass through the thin aluminium layer and enter the crystal in which they generate photons that are

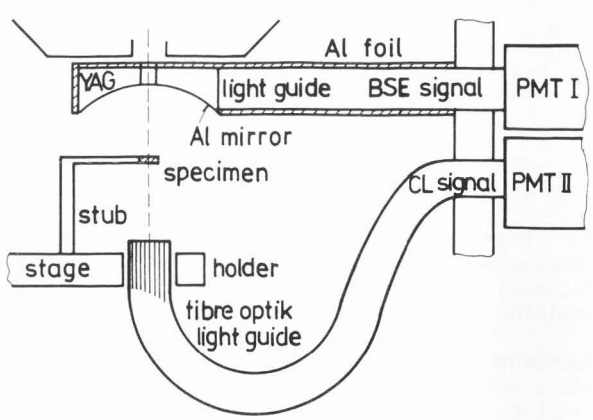

Fig.1. Principle diagram of the CL-BSE detector.

guided by the bulk light guide toward PMT I. This allows the simultaneous recording of the CL and BSE signals.

For the CL signal, neither the BSE detector nor the SE detector can be sources of false light generated by SEs in the scintillator or light guide of the SE detector and propagated into the specimen chamber. The modified ET detector described by Autrata (1990) fully meets this prerequisite. The aluminium coated cone-shaped YAG scintillator together with the input part of the light guide is situated in the detector assembly equipped with an electrooptical diaphragm which prevents possible propagation of light into the specimen chamber. Unlike some SE detectors with powdered scintillators (e.g. Planotec without Al coating), the above mentioned SE detector used for this work eliminates no matter how weak influence of SEs on the CL signal.

The possibility of simultaneous recording of the three image modes suggests that the microscope should be equipped with two additional video channels for the BSE and CL signals, respectively. In the specimen chamber of the microscope, two spare flanges on which the light guides could be mounted, must be available. If on one of these flanges an X-ray spectrometer is mounted, only one flange is left free. In that case, it is possible to integrate in one flange the BSE and the SE detector the signals of which are selected using the optical diaphragm as described by Autrata (1984). Similarly, the CL and the BSE detector can be integrated into one flange. One PMT is used.The signal is selected by shutting or opening the optical diaphragm inserted between the light guides and the PMT.

Geometry and collection efficiency of the YAG mirror CL detector

As evident from Fig. 2, the efficiency of the YAG mirror CL detector depends on the CL light collection efficiency and on the geometrical configuration of the mirror, specimen and the light guide.

The light collection efficiency η (light collected by the spherical mirror) is determined from the ratio of the mirror surface to the surface area delimited by the solid angle of CL radiation amounting to 2π. The efficiency depends on the specimen - mirror distance z_0 and is shown in Fig. 3 for the case when light is propagated homogeneously in all directions over the solid angle 2π (curve 1) and for the case when it is propagated according to the cosine law (curve 2).

The problems connected with the geometrical configuration of the spherical mirror, specimen and light guide are obvious from Fig. 2 and Fig. 4a, b, c. If the specimen is situated in front of the mirror focus F_1 (Fig. 4a), the light beams will be reflected by the mirror at such a large angle that their collection will become impossible. The virtual image of the object in point O lies outside the detection system. If the specimen is situated in the mirror focus F_1 (Fig. 4b) the light beams will be reflected by the mirror in parallel, forming a cylinder the diameter of which is equal to the diameter of the mirror. If the light guide window were to collect all the light beams, its diameter would have to be the same as that of the mirror. As the mirror diameter ranges from 25 to 30 mm (in our case 29.9 mm), this concept is hardly applicable.

The optimum configuration is shown in

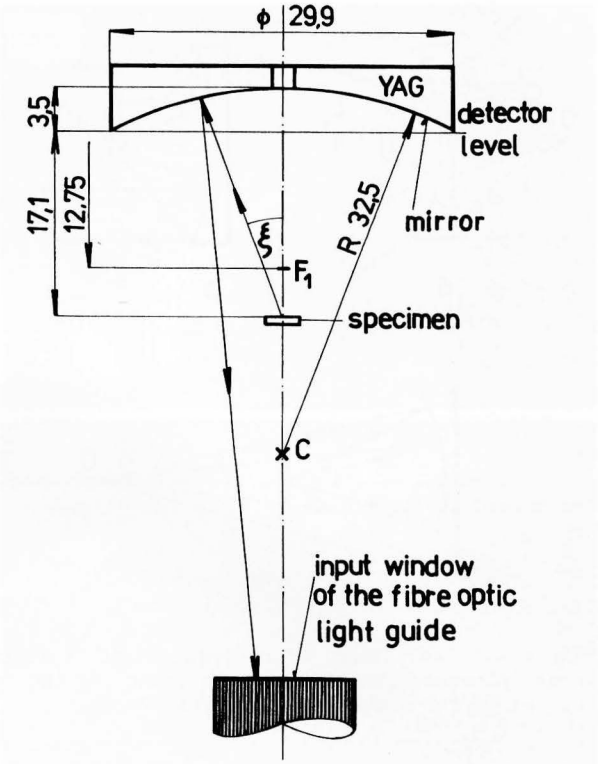

Fig.2. Configuration of the spherical mirror for detection of the CL signal. Distances in mm.

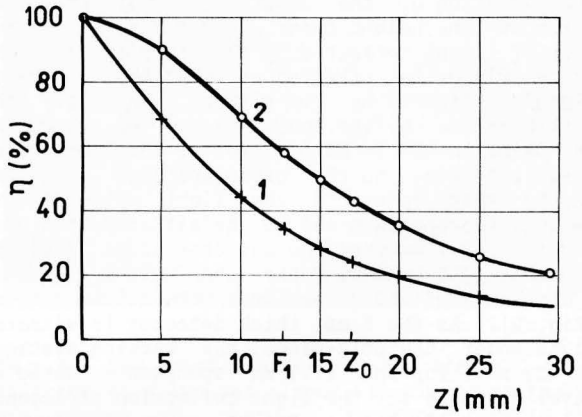

Fig.3. Collection efficiency η versus the specimen - detector level distance z when light is emitted homogeneously (curve 1) and when light is emitted according to the cosine law (curve 2). z_0 denotes the distance used for the detector.

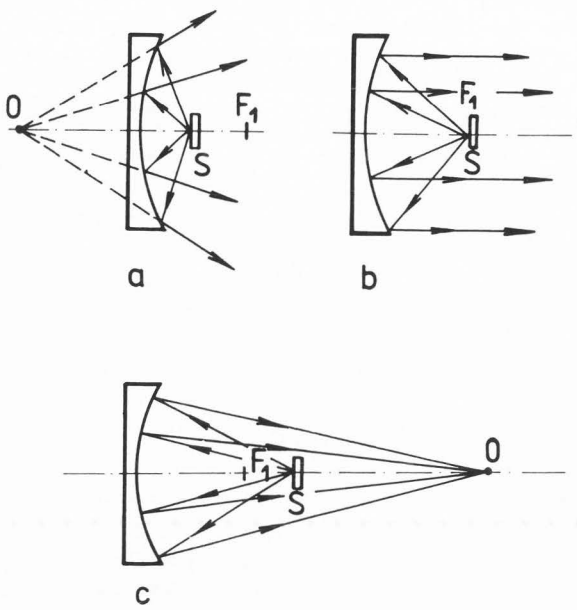

Fig.4. Illustration of reflection of CL light three specimen positions: a) in front of the focus, b) in the focus, c) behind the focus.

Fig. 4c (and also in Fig. 2). The specimen is situated behind the mirror focus F_1. The distance between the mirror focus F_1 and the specimen is a compromise value which allows the achievement of the desired collection efficiency η (Fig. 3) and the location of the input window of the light guide at the height ensuring the maximum collection of light reflected by the mirror. The light guide window is situated so that the entire CL signal reflected by the mirror (except for the part shielded by the specimen) can be trapped by it. Owing to the 13 mm diameter of the light guide used and owing to the given specimen stage geometry that restricts the light guide fixture height, the specimen had to be situated at a distance of 17.1 mm from the detector level, i.e. approximately 5 mm behind the the focus F_1 lying at a distance of 12.7 mm from the detector level (Fig. 2). As the 5 mm thick detector is situated close under the pole-piece, the working distance is 22 mm. For the 17.1 mm specimen - detector level distance z_o the light collection efficiency η is about 40 % (see Fig. 3, curve 2 - cosine law).

The detection efficiency of the YAG mirror CL detector does not depend only on the collection efficiency η but also on the following parameters. The reflectivity of aluminium coated mirrors is not higher than 84 %, so that 16 % of the light signal get lost. A further loss is due to the specimen that shields the reflected light beams. If a 4 x 4 mm specimen held by a bent metal rod is used (Fig. 1), the losses of the light signal propagated in the direction of the light guide that are caused by the specimen shadow amount to 10 % (cosine law). A further 15 % of the light signal get lost in the fibre optic light guide (20 cm long) and the joint between the light guide and the PMT. Summing all these losses, about 20 % of the light emitted from the specimen arrives at the cathode of the PMT. This value approximately corresponds to the detection efficiency of the YAG mirror CL detector. It was compared with the detection efficiency of the simple but sufficiently efficient CL detector designed by Boyde and Reid (1983a, 1983b) amounting to 50 % as reported by Trigg (1985). Similarly, in the case of this Al foil tube detector the losses due to a lower light reflectivity of the Al foil (compared to the evaporated Al layer), the losses due to the imperfectness of the directional light propagation toward the light guide and also a higher efficiency light transfer in the plastic rod-type light guide of a relatively large diameter must be considered. According to our measurement results, the detection efficiency of the YAG mirror CL detector is about half that of the Al foil tube detector.

The detection efficiency of the YAG mirror CL detector can be increased by increasing the collection efficiency, which can be achieved by situating the specimen closer to the mirror focus F_1. This, however, involves increasing the light guide diameter because the reflected light beam has been enlarged.

A more efficient way is to decrease the radius of curvature of the mirror, which leads to a decrease in the focal distance and allows the shortening of the working distance. For example, if the radius of curvature is decreased to 20 mm, then for the mirror of 30 mm in diameter, the specimen - detector level distance z_o can be shortened to 7 mm and the collection efficiency η can be increased to 80 % (cosine law). The 7 mm distance is the limit. At a shorter distance, the SE signal of the SE detector situated in the optimum position begins to decrease. (Our design of the SE assembly allows for the vertical and axial movements of the SE detector).

As a result of the decreased radius of curvature of the YAG mirror, not only the collection efficiency of light but also the collection efficiency of BSEs increase. However in this case, the YAG scintillator does not detect only "high" take-off angle BSEs (material contrast) but also "low" take-off angle BSEs that carry information about the topographic contrast. The resulting image is then a mixture of the material and topographic contrast with a relatively big proportion of the latter. This is the reason why we prefer the detection by the BSE detector in the "high" take-off angle position (despite a decreased signal) and the high resolution in material contrast that cannot be imaged using any other signal mode. (By the way, the topographic BSE contrast can be recorded when the YAG scintillator is shifted aside.)

To obtain a high resolution of the mean atomic number in material contrast without changing the specimen position (a change in the working distance necessitates changing the specimen position) was the reason why the YAG mirror with a radius of curvature of 32.5 mm and with a CL collection efficiency lower than the attainable was designed and built. The configuration shown in Fig. 2 is therefore a compromise made with regard to the detection in both the BSE and SE modes.

Properties of the BSE detector

The collection efficiency $\eta = 40$ % is valid not only for CL but - as it follows from the direction of the trajectories of BSEs - also approximately for them. The high efficiency electron - photon energy transfer in the single crystal YAG scintillator together with the sufficient efficiency of collection of BSEs detected in the "high" take-off angle allows recording of material contrast of two neighboring materials with an atomic number discrimination of 0.1 (atomic number discrimination 0.1 represents the backscatter image contrast of two neighboring materials. One of them has the atomic number 29 and the other 29.1). Owing to the 70 nm thickness of the Al layer forming the mirror on the spherical YAG scintillator, the BSE detector can record an image with a usable signal-to-noise ratio from a primary electron energy of 4 keV upwards.

Light generated in the scintillator is guided toward the PMT using a bulk light guide cemented to one half of the peripheral area of the spherical scintillator disc. Owing to the shape of the scintillator and owing to the way light is collected from the scintillator, the difference in the homogeneity of the signal coming from the scintillator semi-discs opposite and facing the PMT amounts to about 10 %.

The detector is retractable. It can be shifted to a position in which it does not restrict the operation of the x-ray spectrometer. Or it can be situated in the position which allows the side detection of BSEs emitted at a "lower" take-off angle that carry topographic information.

Performance of the integrated CL-BSE detector

Phosphors

Fig. 5 shows images of the luminescent yttrium aluminium garnet (YAG) used in the form of a bigger crystal grain (A), fine crystals (B) and fine crystals on the conducting silver paste substrate (C). The YAG surface was made slightly conductive by applying indium tin oxide using chemical spraying. It is evident from the CL image (CLI) that the YAG is a strong source of CL and the amount of light emitted from it is dependent on the surface relief of the fissile areas the topography of which is clearly seen in the SE image (SEI). The pseudotopographic slight contrast in the CLI is given by different intensities of the excited light in the dependence on the refraction and reflection of the light beams by the crystal grain surface structures. The backscattered electron image (BSI) gives information about the material distribution of the silver paste (brighter areas). Such information cannot be obtained from the SEI. The distribution of fine YAG crystals (B) in the silver paste is evident from the BSI, but it is not sufficiently marked because the sharp topography of the specimen suppresses the material contrast. These crystals can be clearly seen in the CLI.

The charging artefacts (a) due to imperfect conductivity of the surface of the crystal grain (A) are markedly evident from the SEI and essentially less evident from the BSI. The CLI shows that the CL intensity is lower in the place of a bigger charge (evident from SEI).

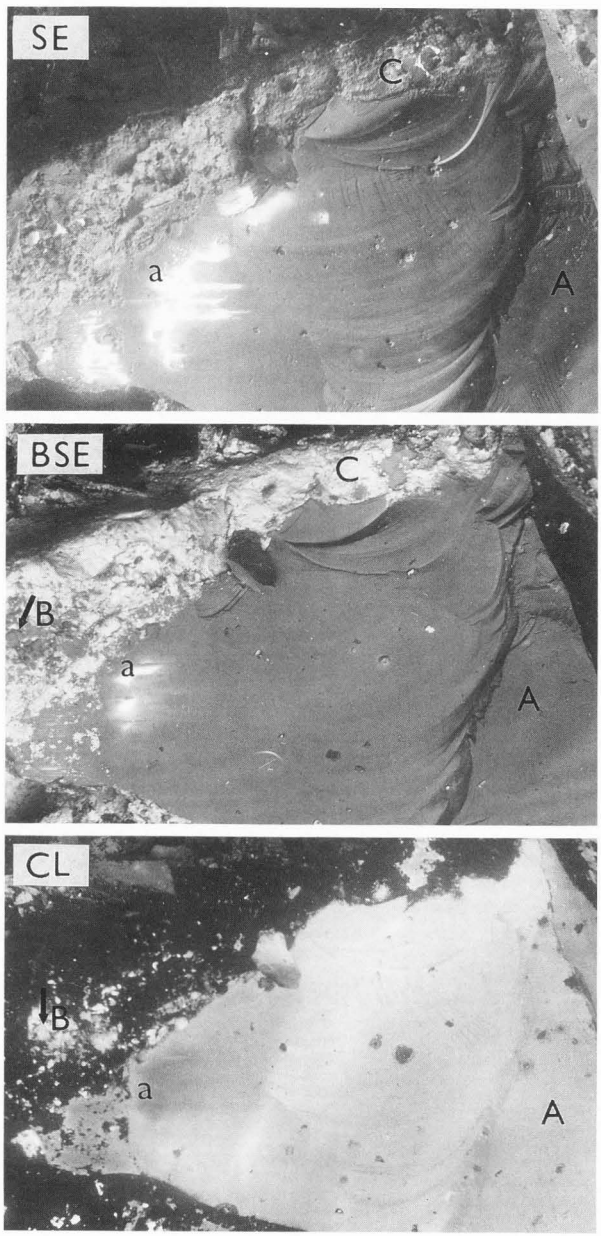

Fig.5. YAG crystal grain (A) and fine YAG crystals (B) (5 - 100 μm) placed in silver paste (C). a - region of charging artefacts, E_o=10 keV, I_o=40 pA, horizontal field width 1 mm.

Insulation plastic materials

The usefulness of observation of several image modes in real time can be illustrated with an example of a dielectric breakdown in polymer insulation materials that are cathodoluminescent in most cases. Fig. 6 is an image of an area of a po-

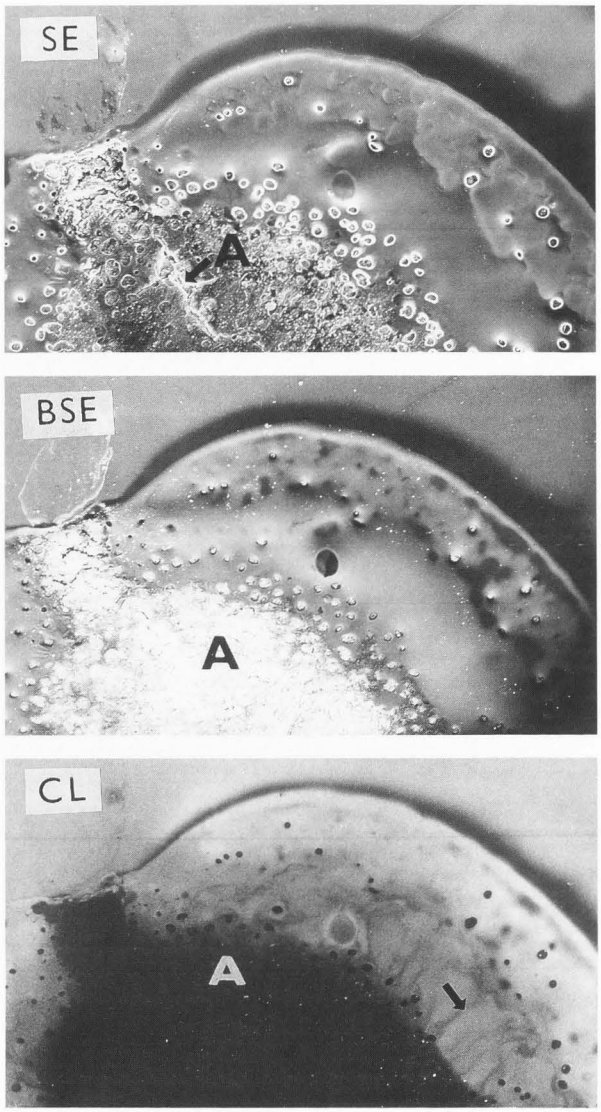

Fig.6. Electrical breakdown through a polyethylene terephthalate foil. E_o=20 keV, I_o=500 pA, horizontal field width 192 μm.

lyethylene terephthalate foil where the high voltage induced breakdown took place. The dark area shown in CLI (A) documents the extinction of the cathodoluminescent properties in the breakdown center. This breakdown center which is shown bright in the BSI (A) informs about the change in the material properties of the plastic over the whole center, whereas the SEI (A) shows only a change in topography with a marked scratch left by the propagated electric charge. The CLI further shows that the extinction of the CL properties becomes evident in the form of striations (see the arrow) caused by a change in material that go from the center outwards. The mentioned changes take place in the range where the concentration changes so slightly (CL intensity changes in the range of concentrations from 10^{-5} to 10^{-6} w%) that it is not possible to use the BSE material contrast for their imaging.

A serious problem connected with plastic materials is a relatively rapid degradation of CL that takes place after primary electron beam irradiation. The degradation rate depends on the radiation dose which among others depends on the electron beam current. To decrease the degradation of CL, it is necessary to work with a low beam current which, however, is not capable of producing a sufficiently high intensity of the CL light. The detection capabilities of a low CL intensity depend on the detection efficiency of the CL system. The decrease in the CL intensity in the area (D) of the polyethylene terephthalate foil after ten-minute illumination by an electron beam with a current of 400 pA is shown in Fig. 7. The undamaged SE image proves that it is not contamination that is shown there but CL degradation that is irreversible.

The influence of the electron beam on the CL intensity can manifest itself not only in a decrease but also in an increase in the CL intensity as is the case with some biological specimens, CL phosphors and others. The causes of these changes depend on the specimen materials and are various.

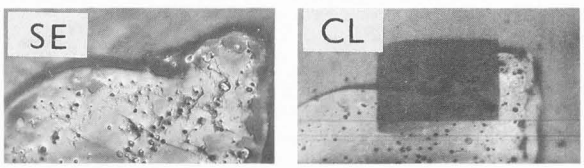

Fig.7. Degradation of CL (exposed area D) after ten-minute electron beam illumination. E_o=20 keV, I_o=500 pA horizontal field width 170 μm.

Textile fibres

The recording of different image modes in real time is especially advantageous when, for example, textile specimens are investigated (Fig. 8). Most cloths are mixtures of fibres from different materials that can show CL of different intensities. The effect of brightening agents or other chemical agents possessing luminescent properties can stain the fibre with a different CL intensity. Then the CL mode together with the BSE mode can identify the material distribution of the fibres or enable one to study other properties of the fibres.

Cloths are electrically insulating materials and a charge is produced on their surface after they are hit by electrons. It is difficult to make the cloth surface conducting. Then the BSI which suffers from the surface charge to a smaller extent is the only source of topographic or material information. From the BSI showing a textile material (Fig. 8) consisting of 30 % polyester fibres and 70 % viscose fibres, it is not possible to distinguish the distribution and the real concen-

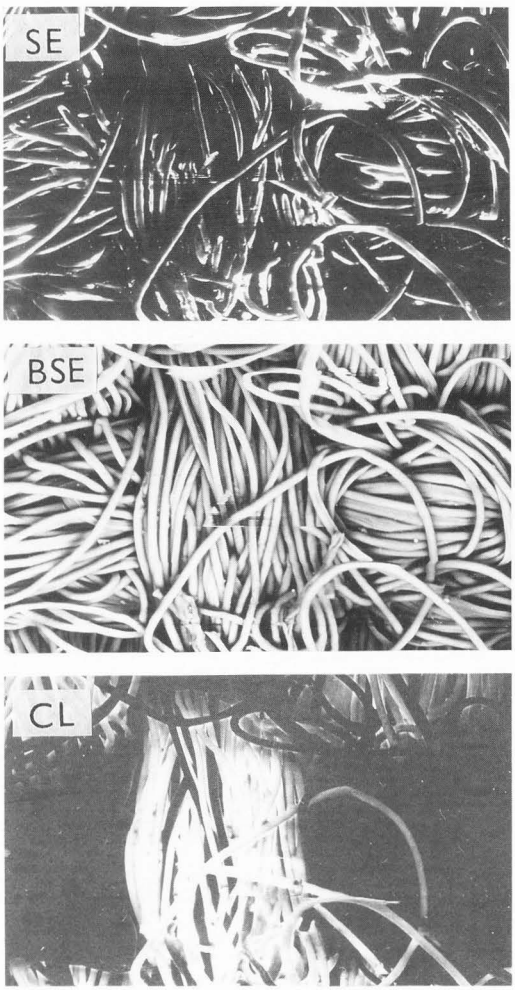

Fig.8. Polyester-viscose cloth, E_o=20 keV, I_o=200 pA, horizontal field width 510 µm.

tration of both kinds of the fibres. Only the CLI allows this. This image shows marked CL of the polyester fibres and negligible CL of the viscose fibres.

Biological specimen

Fig. 9 shows a section of roe-corn dehydrated by air drying. The roe-corn was not embedded in any compound because most embedding compounds are luminescent more or less. No dye was injected into the specimen. From this it follows that the emitted CL is autoluminescent. The surface was made conductive using an antistatic spray that on the one hand restricts the resolution but on the other hand allows a better light transmission. Compared to a 10 nm gold layer, the transmission is two times higher.

For biological specimens, the interpretation of autoluminescence is often very difficult because this kind of luminescence has various causes and the comparison of different image modes can be insufficient for the interpretation of the specimen. From the comparison of the image modes shown in Fig. 9 certain correlations can be observed. Nevertheless, it is impossible to interpret the lawful behavior.

On the one hand, the localities where a lower atomic contrast can be assumed (according to dark places in two circles in the BSI) correspond to the CL localities that are shown in the CLI. On the other hand, some localities where a higher atomic number can be assumed (according to light places marked with a rectangle in the BSI and CLI) are also cathodoluminescent whereas others (those marked with an arrow in the BSI and CLI) are not cathodoluminescent.

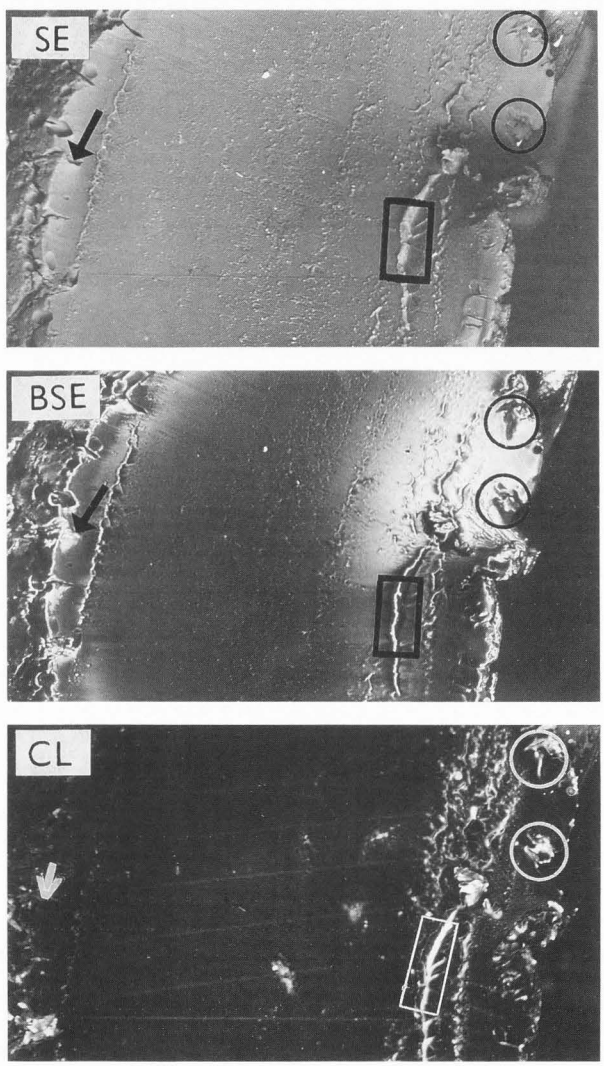

Fig.9. A section of a roe-corn, E_o=7 keV, I_o=500 pA, horizontal field width 126 µm.

Semiconductor specimens

Integral CL, BSE and SE micrographs in Fig. 10 show a number of etched pits together with

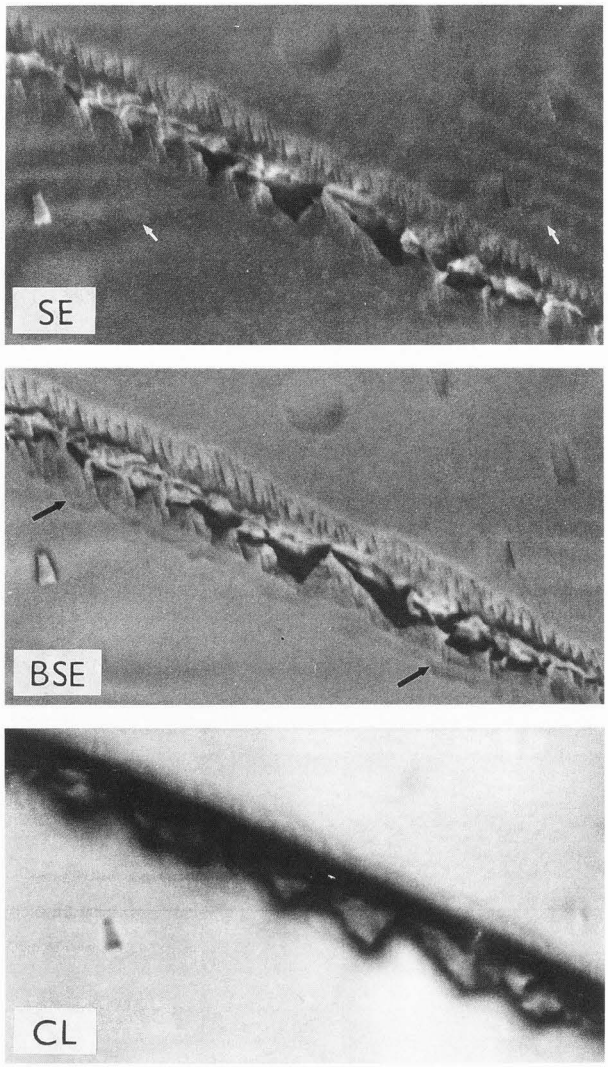

Fig.10. Etched structural defects in InP, E_o=30 keV, I_o=2000 pA, horizontal field width 62 μm.

triangular-shaped dislocations located at a graded layer in a single crystalline InP material doped with Te of 1.10^{-17} cm^{-3} concentration. The InP plate was etched in a mixture of H_3PO_4 and HBr for a period of 5 min.Presumably, a low-angle boundary has been visualized in that way. In addition to the small etched pits observed in the SE and the BSE image, large etched triangular-shaped pits believed to be associated with dislocations became visible. A line of these dislocations is concentrated at the graded layer and grows through the whole volume of the material. With regard to the wavelength of the emitted light with a maximum of 760 nm, the PMT with the S1 photocathode was used in this case. The SE and the BSE image create a useful complementary mode which allows a more precise interpretation of the defective structure.

Acknowledgement

We wish to thank A. Boyde from the University College London for his original idea of the integrated CL-BSE detector that was an inspiration of our work.

References

Autrata R (1984) A Double Detector System for BSE and SE Imaging. Scanning 6:174-182.

Autrata R (1990) A Modification of the ET Secondary Electron Detector with a Single Crystal Scintillator. Scanning 12:119-125.

Balk LJ, Kubalek E, Menzel E (1975) Time resolved and temperature dependent measurement of electron beam induced current (EBIC) and voltage (EBIV) and cathodoluminescence (CL) in the SEM. Scanning Electron Microsc. 1975; I:447-455.

Barnett WA, Jones BL, Wise MLH (1975) Observations on natural and induced cathodoluminescence from vaginal epithelial cells. Micron 6:93-100.

Bond EF, Beresford D, Haggis GH (1974) Improved cathodoluminescence microscopy. J. Microsc. 100:271-282.

Boyde A, Reid SA (1983a) Simple collectors for cathodoluminescence in the SEM made from aluminium foil. J. Microscopy 132:239-242.

Boyde A, Reid SA (1983b) New methods for cathodoluminescence in the scanning electron microscope. Scanning Electron Microsc. 1983; IV:1803-1814.

Bröcker W, Pfefferkorn GE (1978) Bibliography on cathodoluminescence. Scanning Electron Microsc. 1978; I:333/351.

Carlsson L, van Essen CG (1974) An efficient apparatus for studying cathodoluminescence in the scanning electron microscope. J. Phys. E7:98-100.

Davidson SM, Iqbal MZ, Northrop DC (1975) SEM cathodoluminescent studies of plastically deformed gallium phosphide. Phys. stat. sol. (a) 29:571-578.

De Mets M (1974) Improved Cathodoluminescence Detection System. J. Phys. E7:971.

Herbst R, Hoder D (1978) Cathodoluminescence in biological studies. Scanning 1:35-41.

Hörl EM (1978) Cathodoluminescence-actual state of instrumentation. Microsc. Acta 2:236-248.

Hörl EM, Mügschl E (1972) Scanning electron microscopy of metals using light emission. Proc. 5th Eur. Congr. on Electron Microscopy (London: Inst. of Physics) 502-503.

Jones GAC, Gopinath A (1973) Some applications of cathodoluminescence in direct gap semiconductors. SEM: systems and applications, The Inst. of Physics, London-Bristol, 266-271.

Judge FJ, Stubbs JM, Philp J (1974) A concave mirror light pipe photon collecting system for cathodoluminescent studies on biological specimens in the JSM-2 scanning electron microscope. J. Phys. E7:173-174.

McKinney WR, Hough PVC (1977) A new detector system for cathodoluminescence microscopy. Scanning Electron Microsc. 1977; I:251-256.

Rasul A, Davidson SM (1977) SEM measurement of minority carrier lifetimes at dislocations in GaP, employing photon counting. Scanning Electron Microsc. 1977; I:233-240.

Thornton PR (1968) Scanning electron micro-

scopy. Applications to materials and device science, pp 244-277, Chapman Hall, London 1968.

Trigg AD (1985) A high efficiency cathodoluminescence system and its application to optical materials. Scanning Electron Microsc. 1985; III:1011-1022.

Vale BH, Greer RT (1977) SEM cathodoluminescence detection system for transmission optical fluorescence analysis. Scanning Electron Microsc. 1977; I:241-250.

Williams PM, Yoffe AD (1969) Bombardment of Zinc Sulfide Single Crystals with 30 keV Electrons: Light Emission. Radiation Effects 1, 61-64.

Discussion with Reviewers

D.B. Holt: The mirror geometry and production is not clear. Is the whole focussing mirror ground from a YAG single crystal? Could you not make a mirror of larger area of glass, say, with a smaller area YAG crystal inset in it, to intercept only those BSE's giving material contrast?
Authors: As it follows from Figs. 1 and 2, the whole focusing mirror is ground from a YAG single crystal. The area of the YAG mirror can be enlarged by insetting the YAG mirror into a metal spherical mirror ring so that the angle of collection of BSEs does not change and the angle of collection of photons increases. The mirror ring diameter must be, however, chosen with regard to the SE detector. The mirror must not restrict the extraction of SEs - discussion with Radzimski. The extent of modification depends on the position of the SE detector with regard to the specimen.

E. Kubalek and B. Bollig: How did you measure the difference of 10% in the homogeneity of the BSE signal from the scintillator semi-discs opposite and facing the photomultiplier tube? Do you think, this difference enhances the topographic contrast contribution to the BSE signal significantly?
Authors: An electrostatic mirror formed by a negatively biased steel ball was used for the reflection of the primary beam. By scanning the primary beam over the ball it was possible to scan with a reflected beam the interior of the chamber and the surface of a detector (see Fig. 3 in Autrata and Hejna, Scanning 13 (1991) 275). The difference of 10% in the homogeneity of the BSE signal from the scintillator opaque semidiscs opposite and facing the PMT is very small and can have only a slight shadow effect. The topographic contrast contribution is very low because the high take-off angle BSEs hitting one half of the semi-discs are detected. To obtain topographic contrast, electrons with a much lower take-off angle must be detected.

J.B. Pawley: How was the collection efficiency of the new detector measured for BSE and light?
Authors: For light and BSEs, the collection efficiency was evaluated from the geometrical configuration of the detection system and the specimen. A qualified estimation of losses was included. In addition to the evaluation, the relative collection efficiency was measured by investigating the dependence of the signal (anode current of PMT) on changes in the geometrical configuration of the detection system and the specimen when other conditions (beam current, accelerating voltage, voltage supplied to PMT, specimen surface) remained unchanged. The values of the relative collection efficiency obtained for different geometrical configurations proved to be in good agreement with the collection efficiency values evaluated for different geometries.

E.M. Hörl: Back scattered electrons again scattered at the Al-mirror and at other parts of the stage will also hit partly the entrance surface of the fibre optic light guide and will cause there additional CL. Has the contribution of such BSE to the CL-signal been determined?
Authors: A simple experiment was made to evaluate the contribution of such BSEs to the signal. A gold plate was used as a specimen, because gold has a high backscattering coefficient and its CL signal is zero. Using the CL detector, we measured the signal produced by electrons backscattered from the Al mirror and chamber walls and hitting the entrance window of the CL light guide. Even for high beam currents, this CL signal was so low that it was "drowned" in the noise and was, therefore, considered negligible.

E.M. Hörl: In the discussion the detection efficiency I missed the loss of CL-light at the entrance surface of the fibre optic light guide by back reflection. How large is this loss and taking this loss into account how large is then the total detection efficiency of the system?
Authors: Owing to the index of refraction of the light guide amounting to 1.49, all light beams incident on the entrance window of the light guide over angles larger than 42^{o} (critical angle) will be reflected. This fact was taken into account when the geometrical configuration of our detector was designed (Fig. 2). The maximum angle over which the light beams reflected by the mirror can be incident on the entrance window of the light guide, amounted to 23^{o}. Theoretically, no light should be lost by reflection from the entrance window.

Z. Radzimski: How much light will be lost due to a low angle light scattering and shadowing while imaging highly topographic samples, for example a cloth from Fig. 8? What precautions one should take to avoid artifacts in the CL contrast due to these effects?
Authors: With specimens showing high topography, a great amount of CL light is emitted from the specimen over small angles (with regard to the detector) that do not fit the detector of the design described. The total amount of the light signal lost, which depends on the properties of surfaces of individual specimens, has not been measured. The losses can be decreased by increasing the solid angle of collection of the detector or by decreasing the mirror diameter and by positioning the specimen at a shorter distance from the mirror. However, in both cases conditions for the extraction of SEs become worse and the topographic contrast of the BSI is increased to the detriment of the material contrast. The geometrical configuration of the CL-BSE detector described is, therefore, a compromise between a higher quality

of the CL signal and the quality of the SE and BSE signals.

J.B. Pawley: The beam currents used are quite high compared to those used for SE imaging. What factor of the energy deposited in a material like YAG:Ce ends up at the detector PMT? Can anything be done to reduce the amount that never escapes from the specimen surface? (Anti-reflection coatings?)
Authors: Your question has, in fact, three parts.
a) Generally, it cannot be said that it is necessary to use for recording the CL signal beam currents higher than those usual for SE imaging. With some specimens the CL emission is, however, very low and then high beam currents have to be used. The value of the beam current used depends also on the CL detection system efficiency. For the BSE detection, the beam currents are identical with those used for SE imaging. Our integrated detector has two functions but each of them is based on a different physical principle.
b) BSEs are detected on the principle of electron - photon (in the scintillator) - photoelectron (in the PMT) energy conversion. This conversion can be best expressed by the DQE coefficient that for the YAG-BSE detector modified for the maximum light output signal (R. Autrata, R. Hermann, M. Müller: An efficient single crystal BSE detector in SEM, Scanning, in press) amounts to 0.93 (E_o=15 keV). As the integral CL-BSE detector was not modified, its DQE is lower. No precise measurement was made.
c) An amount of light gets lost in the specimen owing to self-absorption. This amount of light never leaves the specimen. Some amount of light can escape from the specimen over an angle that is unsuitable for the detector. An antireflection coating of the specimen can bring an increase in the light output signal, especially for certain angles. However, antireflection coatings can be used only for some kinds of specimens (material plays an important part) and the thickness of the antireflection layer is so high that it prevents low energy electrons from entering the specimen.

Z. Radzimski: Most of the charging, contamination or damage discussed in your paper could be avoided using lower beam current and/or lower beam energy. What are practical limits for this two parameters taking into account acceptable level of SNR?
Authors: The SE and BSE detection efficiency is not decreased owing to the introduction of the CL system. Both detectors have SNR that is sufficient for work also in the range of beam currents of pA and at beam energies >1 keV in the case of the SE detector and >5 keV in the case of the BSE detector. For the CL detector, the acceptable level of SNR depends on the CL signal value, i.e. on the kind of the specimen. Some specimens which show a high CL signal (phosphors, Fig. 5) can be imaged in the CL mode at energies and beam currents currently used in SEM, and a sufficiently high resolution is obtained. Others, for example biological or semiconductor specimens, show a low to very low CL (all remaining specimens used in this work, Figs. 6-10), and the beam current must be corrected in order to obtain an acceptable level of SNR. As for the magnitude of the CL signal, the beam energy is no critical parameter. The SNR depends on the steepness of the curve of the CL signal versus the beam energy that is different for different specimens. The steepness of this curve is in most cases much lower than the steepness of the curve of the CL signal versus the beam current. Taking into account an acceptable level of SNR, the practical limit of the parameters of the beam current and beam energy could be determined for a given specimen only, which is of no practical importance.

D.B. Holt: How does the convenience of simultaneous detection of BSE, CL and SE images compare with use of a retractable CL detector for serial recording of CL, SE and BSE images. Use of a frame grabber would enable one to view the three images simultaneously. This type of system would take less space and probably cost less than yours which requires three video amplifiers and display C.R.T.S.
Authors: The serial recording of CL, SE and BSE images does not allow their observation in real time. The real time recording makes it possible to observe any of the three modes by switching the chosen video channel on the control panel of the microscope. One monitor is sufficient. When the detection modes are switched, the specimen position remains unchanged and the imaged specimen detail remains maintained. The serial recording necessitates removing the CL detector so that the BSEs and SEs can travel in direction of their respective detectors. The simplest CL detectors (PMT lens, light pipe, system designed by Boyde) can be designed as retractable. However, no simple design of a retractable efficient mirror system (similar to the Robinson BSE detector) is known to us. Mostly, the specimen chamber must be opened, the mirror system removed and the BSE detector capable of detecting material contrast inserted. Thereby the specimen position is changed.
It is surely advantageous to use a frame grabber, but not every SEM is equipped with an expensive computer system that, by the way, also requires analog input information from the mentioned three video channels.

D.B. Holt: The arrow in Fig. 6 marks an interesting feature which you call a striation, which does not appear in either the BSE or SE images so your detector does not appear to help identify the striations. I do not understand your discussion of this phenomenon. What is the 'concentration' you mention? From the context and your use of "W%" it might be a change in density? Whatever it is, what is the evidence that there is such a change and that it is responsible for the observed CL striations?
Authors: We do not say that the differences in SE, BSE and CL images will be apparent with all specimens and all surface details. However, also those cases when the image detail can be observed in the CL mode and cannot be markedly seen in the SE or BSE modes can enlarge the scope of information. One example is the striations shown in Fig. 6.
Under striations we understand here specimen localities showing inhomogeneities in physical or chemical properties. For example, it is well known that dopants concentrations in the volume of a single crystal (also a semiconductor one) change during its growth. These changes can become evi-

dent in the form of striations and can be accompanied by a change in CL and other properties. One example of striations in the single crystal of yttrium aluminium garnet doped with Nd is shown in figure 11 below. The difference in dopants concentrations for individual striations amounts to 10^{-5} to 10^{-6} percentage of weight (w%). Thus w% stands for the difference in dopants concentrations that can result in a change in CL properties. Fig. 6 is to illustrate the resistance of multilayer insulating materials to sneak currents. The polyethylene terephthalate surface foil of the insulator shows cathodoluminescent properties. Owing to sneak currents, this foil is removed (burnt down). Material contrast imaged in the BSE mode cannot show in detail the least changes in the surface material. This means that in some places only the CL properties (striations) have changed. The BSE detector is not sensitive enough to record such a small change in material composition (e.g. due to a change in composition of the foundation layer).

J.B. Pawley: Did you note any differences between different materials in the rate at which the CL signal decreased due to radiation damage?
Authors: Yes, we did. With some biological specimens and plastic materials the CL signal decreased with increasing radiation dose, whereas with some semiconductor specimens the signal increased with increasing radiation dose. This phenomenon was connected with the dopants concentration. For example, undoped InP showed a decrease in the CL signal, whereas InP doped with 1.0×10^{19} Ge atoms cm^{-3} showed a slight increase in the CL signal and a higher contrast of dopant striations. For some inorganic single crystals (e.g. ZnS), the CL signal also increased with increasing time of radiation, whereas for quartz glass the CL signal decreased. We arrived at a conclusion that it is very difficult to establish a general rule of the influence of radiation damage on the CL signal. It can differ for different specimens and depends on the kind of the specimen structure and its surface.

D.B. Holt: Which causes are responsible for the observed dark patch in your CL images of plastic insulating material, after irradiation. Can you give examples? Is anything known about this phenomenon?
Authors: A great number of plastic materials are cathodoluminescent. Polystyrene, polymethyl-methacrylate, polyester, and polyethylene are examples of plastic materials whose cathodoluminescent properties decrease relatively rapidly after irradiation. The extent of change in CL properties depends on the radiation dose. For example, if a radiation dose of 2.25 MRad/h is applied to the polymethyl-methacrylate scintillator, its light output strength decreases to one half in one hour (Pawley: Scanning Electron. Microsc. (1974), 27-34; Odham et al.: J. Inst. Nuc. Eng. 12 (1971), 4-6). This phenomenon is connected with the degradation of macromolecules, with a decrease in the molecular weight of the polymer and with the release of some groups of radicals that extinguish luminescence.

Fig.11. Striations in single crystal of yttrium aluminium garnet doped with Nd.

E. Kubalek and B. Bollig: In your discussion of the semiconductor specimen you state that the complementary mode created by SE image and BSE image allows a more precise interpretation of the defective structure. Can you please explain more detailed the gain of precision in case of figure 10?
Authors: The term "more precise interpretation" is too bombastic for the comparison of the mentioned three image modes. Perhaps it would have been more appropriate to say that in the BSE image some details (marked with the black arrow) are more clearly visible than in the SE image and, in turn, the SE image shows some details (marked with the white arrow) that are not visible in the BSE image.

D.B. Holt: Your SE shows what appear to be two rows of etch pits running from top left to bottom right, diagonally across the field of view. You appear to believe the large triangular pits in the lower row only correspond to dislocations. Why?
Authors: Yes, we do. All three images illustrate one or more rows of etched pits. It might be a case of a low-angle boundary that became visible as a growth defect in the InP single crystal. The triangular pits were termed dislocations according to the triangular-shaped dislocations typical of the InP and other semiconductor materials (e.g. Patel A.R., Desai C.C., Z. Kristallogr. 121, 55 (1965), Joshi M.S.,Kotru P.N., Ittyachen M.A.: Kristalografia 15 (1970) 103). However, the denotation remains on the level of an assumption. It would be possible to specify the defect more precisely by diffraction topography. As we did not make any experiment to prove this, it is more appropriate to name it defective structure instead of dislocations.